Prediction of Approximate Transition States by Bell–Evans–Polanyi Principle: II. Gas Phase Unimolecular Decomposition of Methyldioxirane

JOSEP MARIA ANGLADA,[1] EMILI BESALÚ,[2] JOSEP MARIA BOFILL,[3] RAMON CREHUET[1]

[1] *Institut d'Investigacions Químiques i Ambientals, CID–CSIC, Barcelona, Catalunya, Spain*
[2] *Institut de Química Computacional i Departament de Química, Universitat de Girona, Girona, Catalunya, Spain*
[3] *Departament de Química Organica i Centre Especial de Recerca en Química Teòrica, Universitat de Barcelona, Martí i Franquès 1, E-08028 Barcelona, Catalunya, Spain*

Received 15 January 1999; accepted 17 March 1999

ABSTRACT: We apply a model of the Bell–Evans–Polanyi principle (BEP) proposed in the accompanying article (Part I) and CASSCF wave functions to locate approximate transition structures for the unimolecular decomposition of methyldioxirane (**1**) into methyldioximethane (**2**) and **2** into acetic acid (**3**), formyl acetate (**4**), and $CO_2 + CH_4$ (**5**), respectively. The model provides very good starting geometries for the transition structure search except for the dissociation step into $CO_2 + CH_4$. In this case, the minimum crossing point of the interaction between the two quadratic surfaces centered in **2** and $CO_2 + CH_4$ is an acceptable starting point for the transition state search. The contribution weights of reactants and products to the transition structure are given in the context of this method. In addition, the relative activation energies are provided at the CASSCF and CCSD(T) levels of theory. J Comput Chem 20: 1130–1137, 1999

Keywords: transition state location; BEP model; methyldioxirane decomposition

Correspondence to: J. M. Bofill; e-mail: jmbofill@qo.ub.es and J. M. Anglada; e-mail: anglada@qteor.cid.csic.es

Contract/grant sponsor: Spanish DGICYT
Contract/grant numbers: PB95-0278-CO2-01; PB95-0278-C02-02
Contract/grant sponsor: CIRIT

CCC 0192-8651 / 99 / 111130-08

Introduction

In part I of this study,[1] we presented a model based on the Bell–Evans–Polanyi (BEP) principle, which provides good starting geometries for the transition state (TS) search. Moreover, the method also provides a way to assign a contribution of weights of reactants and products to the TS in the context of this method. In this study, we apply this method to the study of gas phase unimolecular decomposition modes of methyldioxirane (**1**). The gas phase unimolecular decomposition of **1** has a direct interest in atmospheric chemistry, because **1** is an intermediate in the unimolecular decomposition of acetaldehyde carbonyl oxide. This is one of the products resulting from the ozonolysis of alkenes,[2–6] according to the Criegee mechanism.[7] The unimolecular decomposition of **1** corresponds to the so-called ester channel and involves reactions (1)–(4) (Fig. 1).[8–12]

Reaction (1) corresponds to the ring opening process of **1** that produces methyldioximethane (**2**). Reactions (2)–(4) involve different paths of **2** decomposition, yielding acetic acid (**3**), formyl acetate (**4**), and CO_2 + CH_4 (**5**), respectively. Previous theoretical results for these reactions as well as for the parent dioxirane have been reported recently in the literature.[13–19]

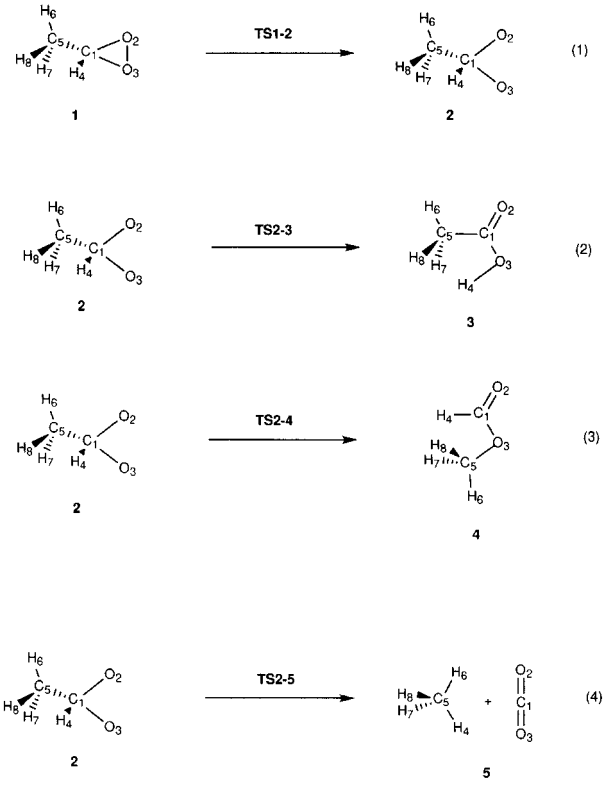

FIGURE 1.

Technical Details of Calculations

The geometry of the stationary points on the potential energy surface (PES) has been determined by using the CASSCF wave functions.[20] The active space was selected according to the fractional occupation of the natural orbitals (NOs)[21] generated from the first-order density matrix calculated from a MRD-CI[22–24] wave function, correlating all valence electrons. The selection procedure provides a common active space of ten electrons in nine orbitals [CASSCF(10, 9)] for all stationary structures except **2** and **TS2**–**5**, where the selection procedure leads to a CASSCF(8, 8) active space. For these structures, the CASSCF(10, 9) wave function leads to incorrect molecular geometries with a different CO bond distance for each CO bond. However, to make the CASSCF energies comparable, we have also performed a single point CASSCF(10, 9) calculation at the **2** and **TS2**–**5** optimized geometries. All CASSCF stationary points were also characterized and the corresponding zero point vibrational energies (ZPVEs) values were scaled by 0.8929.[25] The CASSCF calculations were done using the split-valence-polarized 6-31G(d, p) basis set.[26]

As a starting point for the TS search we have used geometries obtained by modeling of the BEP principle described in part I. The corresponding geometrical parameters for each of the reactions (1)–(4) are collected in Tables I–IV. For each reaction, the prefix **CP** stands for the minimum crossing point of the interaction between the two quadratic surfaces centered in reactants and products, respectively, **TSa** is the transition geometry obtained by using option 3A in the BEP model, **TSb** is the transition geometry obtained by using option 3B in the BEP model, and **TS** corresponds to the CASSCF transition structure. One should note from the previous study that, in option 3A of the model, the Hessian matrix at the CP geometry is that of the real PES (computed at the CASSCF level of theory in this case), whereas, in option 3B, the Hessian matrix is approximated from the Hes-

TABLE I.
Energies (in Hartree) and Geometrical Parameters (Distances in Angstroms and Angles in Degrees) of Methyldioxirane (1), Methyldioxymethane (2), Crossing Point (CP1–2), Transition State of the BEP Model (TSa1–2 and TSb1–2), and of Actual Surface (TS1–2), for Reaction (1).

	1	2	CP1–2	TSa1–2[a]	TSb1–2[b]	TS1–2
Energy	−227.80677	−227.77816[c]	−227.74230[d]	−227.77172[e]	−227.77668	−227.76824
O_2C_1	1.405	1.390	1.388	1.423	1.451	1.408
O_3C_1	1.405	1.390	1.389	1.416	1.491	1.402
$O_3C_1O_2$	67.3	116.0	90.1	100.3	93.1	99.9
H_4C_1	1.079	1.087	1.080	1.084	1.077	1.086
$H_4C_1O_3$	114.3	107.2	111.5	109.5	113.9	107.4
$H_4C_1O_3O_2$	107.5	119.7	114.5	115.5	113.9	118.3
C_5C_1	1.523	1.565	1.514	1.537	1.499	1.547
$C_5C_1H_4$	116.9	110.6	114.3	112.7	116.8	111.6
$C_5C_1H_4O_3$	−142.6	−117.4	−130.7	−126.3	138.3	−127.0
H_6C_5	1.082	1.083	1.082	1.083	1.082	1.082
$H_6C_5C_1$	109.3	109.5	109.7	109.6	109.8	109.5
$H_6C_5C_1O_2$	−38.5	−63.0	−51.3	−57.4	−44.2	−56.1
H_7C_5	1.085	1.081	1.083	1.084	1.087	1.084
$H_7C_5C_1$	109.8	109.0	109.4	109.2	110.0	110.5
$H_7C_5C_1O_2$	81.8	56.7	68.9	62.4	75.9	64.7
H_8C_5	1.085	1.081	1.084	1.084	1.081	1.084
$H_8C_5C_1$	109.8	109.0	109.2	109.7	108.7	108.7
$H_8C_5C_1O_2$	201.1	177.2	188.7	182.3	195.6	184.4

[a] Transition state of the BEP model obtained using option 3A.
[b] Transition state of the BEP model obtained using option 3B.
[c] CASSCF(10, 9) energy at CASSCF(8, 8) optimized geometry. The CASSCF(8, 8) energy is −227.77424 hartree.
[d] The CASSCF(10, 9) energy at this point is −227.780431 hartree.
[e] Corresponding to the energy obtained according to the BEP model following option 3A. At this point, the CASSCF(10, 9) energy is −227.76721 hartree.

sian matrices of the reactants and products, respectively. The latter is much less expensive, but the applicability range is given by the s value of eq. (8) in previous article.

Finally, we also considered the effect of the dynamical valence-electron correlation on the relative energies of the CASSCF-calculated stationary points by performing single point calculations using CCSD(T).[27–29] The 6-311G(2df, 2p) basis set[30,31] was used in these calculations. Structures **TS1–2**, **2**, **TS2–3**, **TS2–4**, and **TS2–5** have a clear biradical character and, therefore, the CCSD(T) calculations were based on a reference UHF wave function of broken symmetry. For these cases, the $\langle S^2 \rangle$ expectation value of the UHF wave function is about 1 and about 0.12 after spin projection.

The CASSCF calculations were carried out by using the GAMESS[32] program package and the CCSD(T) computations were done with the GAUSSIAN-94[33] system of programs.

Results and Discussion

REACTION (1)

The first step in the unimolecular decomposition of methyldioxirane (**1**) is the ring opening process yielding methyldioximethane (**2**), with both structures possessing C_s symmetry. **1** is characterized mainly by a closed-shell structure, which is described by the electronic configuration $\ldots 10a'^2 11a'^2 4a''^2 5a''^2$. This electronic state has 4π electrons in the COO ring, which correspond to the π (OO) bond and to the π (COO) bond and is designated as $(^1A', 4\pi)$ state. On the other hand, **2** has a clear biradical character. It is described by the mixing of the electronic configurations $\ldots 10a'^2 4a''^2 5a''^2 6a''^2 - \ldots 10a'^2 11a'^2 4a''^2 6a''^2$ and possesses 2π electrons in the COO moiety. Consequently, it is designated $(^1A', 2\pi)$. As occurs in the case of the parent dioxirane,[17,34,35] the $(^1A', 2\pi)$

TABLE II.
Energies (in Hartree) and Geometrical Parameters (Distances in Angstroms and Angles in Degrees) of Methyldioxymethane (2), Acetic Acid (3), Crossing Point (CP2–3), Transition Structure of BEP Model (TSa2–3), and of Actual Surface (TS2–3), for Reaction (2).

	2	3	CP2–3	TSa2–3	TS2–3[a]
Energy	−227.77816[b]	−227.94271	−227.73436[c]	−227.74578[d]	−227.77465
O_2C_1	1.390	1.209	1.297	1.226	1.316
O_3C_1	1.390	1.368	1.378	1.366	1.380
$O_3C_1O_2$	116.0	120.1	104.8	114.8	121.9
H_4C_1	1.087	1.918	1.254	1.253	1.165
$H_4C_1O_3$	107.2	27.4	87.3	81.4	84.3
$H_4C_1O_3O_2$	119.7	180.0	136.9	138.7	96.6
C_5C_1	1.565	1.513	1.516	1.535	1.520
$C_5C_1H_4$	110.6	87.6	103.6	99.8	113.7
$C_5C_1H_4O_3$	−117.4	180.0	−113.9	−109.1	−114.3
H_6C_5	1.083	1.080	1.080	1.073	1.084
$H_6C_5C_1$	109.5	109.4	109.4	108.9	109.0
$H_6C_5C_1O_2$	−63.0	0.0	−60.6	−66.2	−74.0
H_7C_5	1.081	1.087	1.085	1.087	1.081
$H_7C_5C_1$	109.0	110.5	109.5	109.0	110.2
$H_7C_5C_1O_2$	56.7	120.0	58.8	53.4	45.0
H_8C_3	1.081	1.087	1.081	1.084	1.081
$H_8C_5C_1$	109.0	110.5	109.4	109.4	110.2
$H_8C_5C_1O_2$	177.2	240.0	178.8	173.0	166.9

[a] Other parameters of interest are r(H_4O_3) = 1.714 Å and ∠($H_4O_3C_1$) = 42.5°.
[b] CASSCF(10, 9) energy at CASSCF(8, 8) optimized geometry. The CASSCF(8, 8) energy 1 is −227.77424 hartree.
[c] The CASSCF(10, 9) energy at this point is −227.74188 hartree.
[d] The CASSCF(10, 9) energy at this point is −227.73926 hartree.

state is a low-lying electronic state of the $(^1A', 4\pi)$ state, and it is originated from a double excitation from the π system in the COO ring to the antibonding σ^* (OO) orbital ($10a'^2 \rightarrow 6a''^2$ and $5a''^2 \rightarrow 6a''^2$). Moreover, close to the transition state connecting **1** $(^1A', 4\pi)$ and **2** $(^1A', 2\pi)$, an avoided crossing occurs, so that $(^1A', 2\pi)$ is the lowest electronic state in the open form. Consequently, this reaction constitutes a very fine example with which to illustrate our BEP model. The results obtained are displayed in Table I. The starting point in looking for the transition state structure is the CP. Using the BEP model option 3A (see part I), we obtained a converged geometry of the transition state (**TSa1–2**) that is very close to that of the real transition state (**TS1–2**). Moreover, the transition energy predicted by the BEP model is also very close to that of the real transition state with a difference of only 2.2 kcal/mol between both values. The contribution weights of the reactants and products in **TSa1–2** are $(c_1)^2 = 0.05$ and $(c_2)^2 = 0.95$, which means that only **2** contributes to **TSa1–2**. These values are practically the same [$(c_1)^2 = 0.04$ and $(c_2)^2 = 0.96$] as those corresponding to the real transition structure **TS1–2** and also agree with the structure of the electronic wave function ($0.74 \ldots 10a'^2 4a''^2 5a''^2 6a''^2 - 0.51 \ldots 10a'^2 11a'^2 4a''^2 6a''^2$), very close to that of **2** ($0.76 \ldots 10a'^2 4a''^2 5a''^2 6a''^2 - 0.62 \ldots 10a'^2 11a'^2 4a''^2 6a''^2$).

BEP model option 3B is much less expensive and, in this case, is also applicable, because the s parameter of eq. (8) of the preceding study has a value of 0.92. With this option we obtained a converged geometry of the transition state **TSb1–2** of lower quality than that obtained using option 3A, although it also represents a very good starting point for the search of the real transition structure. On the other hand, the contribution weights of the reactants and products in **TSb1–2** are $(c_1)^2 = 0.28$ and $(c_2)^2 = 0.72$, values that are far from those of the real transition structure (see earlier).

REACTION (2)

Reaction (2) involves the H_4 migration from C_1 to O_3 and a rotation of the methyl group. Both **2**

TABLE III.
Energies (in Hartree) and Geometrical Parameters (Distances in Angstroms and Angles in Degrees) of Methyldioxymethane (2), Methylformiate (4), Crossing Point (CP2–4), Transition Structure of BEP Model (TSa2–4), and of Actual Surface (TS2–4), for Reaction (3).

	2	4	CP2–4	TSa2–4	TS2–4[a]
Energy	−227.77816[b]	−227.91592	−227.73029[c]	−227.76142[d]	−227.76927
O_2C_1	1.390	1.208	1.251	1.274	1.286
O_3C_1	1.390	1.326	1.297	1.358	1.366
$O_3C_1O_2$	116.0	123.0	118.1	125.6	124.0
H_4C_1	1.087	1.094	1.079	1.110	1.086
$H_4C_1O_3$	107.2	113.9	120.7	112.8	112.6
$H_4C_1O_3O_2$	−119.7	180.0	−149.6	−147.2	−149.2
C_5C_1	1.565	2.356	1.836	1.717	1.741
$C_5C_1H_4$	110.6	80.5	86.1	93.4	103.8
$C_5C_1H_4O_3$	−117.4	0.0	87.2	92.9	95.1
H_6C_5	1.083	1.078	1.083	1.074	1.075
$H_6C_5C_1$	109.5	136.1	109.1	100.0	107.6
$H_6C_5C_1O_2$	−63.0	0.0	16.0	11.8	61.1
H_7C_5	1.081	1.083	1.078	1.070	1.076
$H_7C_5C_1$	109.0	94.5	118.8	107.4	101.7
$H_7C_5C_1O_2$	−56.7	−124.7	−112.1	−105.1	−57.3
H_8C_5	1.081	1.083	1.084	1.070	1.074
$H_8C_5C_1$	109.0	94.5	98.4	112.4	107.8
$H_8C_5C_1O_2$	177.2	124.7	129.8	130.2	183.5

[a] Other parameters of interest are $r(C_5O_3) = 2.200$ Å and $\angle(O_3C_5C_1) = 38.4°$.
[b] CASSCF(10, 9) energy at CASSCF(8, 8) optimized geometry. The CASSCF(8, 8) energy is −227.77424 hartree.
[c] The CASSCF(10, 9) energy at this point is −227.74274 hartree.
[d] Corresponding to the energy obtained according to the BEP model following option 3A. At this geometry, the CASSCF(10, 9) energy is −227.75814 hartree.

and **3** structures possess C_s symmetry, but the symmetry planes are perpendicular to each other. Table II shows that the CP geometry has an $O_3C_1O_2$ angle of 104.8°, which is shorter than the corresponding angle in **2**; that is, the angle change predicted by the crossing point of the intersection of the two quadratic surfaces has gone in the wrong direction (compare with the real transition structure **TS2–3** in Table II). The CASSCF Hessian has only one negative eigenvector and the BEP model predicts a better starting geometry (**TSa2–3**) for the transition structure search. The contribution weights of the reactants and products in **TSa2–3** are $(c_2)^2 = 0.88$ and $(c_3)^2 = 0.12$, whereas the corresponding weights obtained for the real transition structure (**TS2–3**) are $(c_2)^2 = 0.99$ and $(c_3)^2 = 0.01$, which means that, according to this BEP model, the **TS2–3** presents a very strong contribution of **2**. Because the reaction is highly exothermic (see Table V), we conclude that this reaction obeys the Hammond postulate.[36]

REACTION (3)

Reaction (3) involves the methyl migration from C_1 to O_3 in **2** together with a rotation of the methyl group to produce **4**. Both structures **2** and **4** possess C_s symmetry, but the symmetry planes are perpendicular to each other. At the CP geometry, the *s* parameter of eq. (8) from part I has a value of 0.29 which indicates that only BEP option 3A is suitable in this case. The CASSCF Hessian matrix at the CP geometry has two negative eigenvalues. One of them corresponds to C_5O_3 stretching, whereas the other corresponds to a methyl rotation. In the optimization process, the Hessian matrix was forced to have only one negative eigenvalue and the optimization was stopped with a gradient norm of 0.015 hartree $Å^{-1}$. The geometries displayed in Table III clearly indicate that the **TSa2–4** obtained from the BEP model is a better starting point than the geometry of the crossing point intersection between the two quadratic sur-

TABLE IV.

Energies (in Hartree) and Geometrical Parameters (Distances in Angstroms and Angles in Degrees) of Methyldioxymethane (2), $CO_2 + CH_4$ (5), Crossing Point (CP2–5), and Transition Structure of Actual Surface (TS2–5), for Reaction (4).

	2	$CO_2 + CH_4$	CP2–5	TS2–5
Energy	−227.77816[a]	−227.95028	−227.47434[b]	−227.76200[c]
O_2C_1	1.390	1.159	1.268	1.279
O_3C_1	1.390	1.159	1.266	1.279
$O_3C_1O_2$	116.0	180.0	143.6	132.5
H_4C_1	1.087	3.003	1.103	1.121
$H_4C_1O_3$	107.2	90.0	97.5	112.2
$H_4C_1O_3O_2$	119.7	0.0	−125.1	158.5
C_5C_1	1.565	3.487	2.078	1.769
$C_5C_1H_4$	110.6	17.2	24.8	72.9
$C_5C_1H_4O_3$	−117.4	−90.0	−74.2	−98.4
H_6C_5	1.083	1.078	1.085	1.073
$H_6C_5C_1$	109.5	56.9	106.5	98.2
$H_6C_5C_1O_2$	−63.0	−90.0	−62.9	−70.8
H_7C_5	1.081	1.083	1.153	1.073
$H_7C_5C_1$	109.0	125.0	125.5	106.4
$H_7C_5C_1O_2$	56.7	0.0	62.0	47.3
H_8C_5	1.081	1.083	1.141	1.073
$H_8C_5C_1$	109.0	125.0	119.7	106.5
$H_8C_5C_1O_2$	177.2	180.0	177.6	171.2

[a] CASSCF(10, 9) energy at CASSCF(8, 8) optimized geometry. The CASSCF(8, 8) energy is −227.77424 hartree.
[b] Energy of the crossing point between the two quadratic surfaces. At this geometry, the CASSCF(10, 9) energy is −227.75525 hartree.
[c] CASSCF(10, 9) energy at CASSCF(8, 8) optimized geometry. The CASSCF(8, 8) energy is −227.74529 hartree. Other parameters of interest are $r(C_5H_4)$ = 1.795 Å and $< (C_5H_4C_1)$ = 70.4° and $< (H_6C_5H_4C_1)$ = 180.0°.

TABLE V.

Zero Point Vibrational Energies[a] (ZPVE, in Kilocalories per Mole), Total Energies (*E*, in Hartree), and Relative Energies[b] (ΔE, in Kilocalories per Mole) for Stationary Points Pertaining to Unimolecular Decomposition of Methyldioximethane (1).

	ZPVE	*E*(CASSCF)/ 6-31G(d, p)	*E*(CCSD(T))/ 6-311G(2df, 2p)	ΔE(CASSCF)/ 6-311G(d, p)	ΔE(CCSD(T))/ 6-311G(2df, 2p)
1	33.8	−227.80676	−228.58413	0.0 (0.0)	0.0 (0.0)
TS1–2	34.3	−227.76884	−228.53911	23.8 (24.3)	28.3 (28.8)
2	34.7	−227.77816[c]	−228.55331	17.9 (18.9)	19.3 (20.3)
TS2–3	32.6	−227.77465	−228.54902	20.2 (19.0)	22.0 (20.9)
3	36.8	−227.94271	−228.71996	−85.3 (−82.3)	−85.2 (−82.2)
TS2–4	33.8	−227.76927	−228.54682	23.5 (23.5)	23.4 (23.4)
4	36.6	−227.91592	−228.69451	−68.5 (−65.6)	−69.3 (−66.4)
TS2–5	32.9	−227.76200[c]	−228.54491	28.1 (27.2)	24.6 (23.7)
$CO_2 + CH_4$	30.8[d]	—	−228.74469[d]	—	−100.8 (−103.7)

[a] Obtained at the CASSCF/6-31G(d, p) level of theory and scaled by 0.8929.
[b] Values in parentheses are ZPVE corrected.
[c] CASSCF(10, 9) energy at CASSCF(8, 8) optimized geometry.
[d] Corresponds to the sum of the values obtained for CH_4 and CO_2 separately. CH_4 optimized at the CASSCF(8, 8) level of theory and the computed CASSCF and CCSD(T) energies are −40.28389 and −40.43049 hartrees, respectively. CO_2 optimized at CASSCF(10, 9) level of theory and the computed CASSCF and CCSD(T) energies are −187.76702 and −188.31420 hartrees, respectively.

faces (**CP2–4**) in the search for the real transition structure. The main difference between the **TSa2–4** geometry and the real **TS2–4** involves a rotation of about 40° in the methyl group, whereas the remaining parameters agree quite well (see Table III). The contribution weights of the reactants and products in **TSa2–4** are $(c_2)^2 = 0.60$ and $(c_4)^2 = 0.40$. These values compare with those obtained for the real transition structure **TS2–4** [$(c_2)^2 = 0.59$ and $(c_4)^2 = 0.41$]. Finally, the BEP model predicts an energy for **TSa2–4** that is only 4.9 kcal/mol more energetic than the real CASSCF energy of **TS2–4**, and this value is quite acceptable if we take into account that both structures differ essentially in a rotation of the methyl group.

REACTION (4)

Reaction (4) corresponds to the dissociation of **2** into CH_4 plus CO_2 and takes place through a concerted mechanism that involves a synchronous breaking of the C_1H_4 and C_1C_5 bonds along the formation of the C_5H_4 bond and the two COπ-bonds. This corresponds to the most critical step, because it involves a dissociation process and the products cannot be strictly represented by a quadratic function. In this case, we have taken, as the geometry of the products, the geometry of CH_4 plus that of CO_2 as a supermolecule, where the distances between C_1H_4 and C_1C_5 are close to the sum of the van der Waals radii, respectively (see Table IV), and all eigenvalues of the corresponding Hessian matrix forced to be positive. The CP geometry of the intersection between the two quadratic surfaces is an acceptable starting point for the search for the real transition state (see Table IV). The CASSCF Hessian at the CP geometry has only one negative eigenvalue and the corresponding eigenvector is in the desired direction. Thus, the search of the real transition state **TS2–5** starting from the CP geometry was successful. However, our BEP model has failed in this case to predict a better starting point. Finally, the contribution weights of the reactants and products in the real transition structure **TS2–5** are $(c_2)^2 = 0.99$ and $(c_5)^2 = 0.01$, which means that, according to this BEP model, **TS2–5** presents a very strong contribution of **2**. As in the previous two cases, the reaction is highly exothermic (see Table V) and, consequently, we conclude that it obeys the Hammond postulate.[36]

At this point it is interesting to compare our CASSCF geometrical parameters with those reported very recently by Cremer et al.[18] obtained at the B3LYP level of theory. In general, the results obtained by both methods agree qualitavively, with differences of between 0.01 and 0.07 Å for bond lengths and between 2° and 6° for bond angles.

RELATIVE ENERGIES

For the sake of completeness, we also report, in Table V, the total and relative energies for the unimolecular decomposition of methyl dioxirane (**1**), computed at both CASSCF/6-31G(d, p) and CCSD(T)/6-311G(2df, 2p) levels of theory. The CASSCF relative energies compare with those computed at the CCSD(T) level of theory, and the largest differences are in the **TS1–2**, which is predicted to be 4.5 kcal/mol more stable by the CASSCF wave function and the **TS2–5**, predicted to by 3.5 kcal/mol more stable by the CCSD(T) level of theory. At both levels of theory, the limiting step is the **1** → **2** ring opening process. At this point it is also helpful to compare these results with the recent values reported in the literature and computed at the B3LYP/6-31G(d, p) level of theory.[18] The relative energies also compare qualitatively, and the largest difference is the relative stability of methyldioximethane (**2**), which is reported to be 11.2 kcal/mol at B3LYP level of theory and 17.9 and 19.3 kcal/mol at the CASSCF and CCSD(T) levels of theory, respectively. Moreover, the B3LYP relative energies for the decomposition of **2** compare quite well with the CASSCF and CCSD(T) corresponding values.

Conclusions

In this article we have used the BEP model described previously to study the different decomposition modes of methyldioxirane (**1**). For reactions (1)–(3), the model predicts good starting geometries for the search of the transition structures. These geometries are better than those predicted by the minimum crossing point of the interaction between the two quadratic surfaces centered in reactants and products, respectively. Reaction (4) involves a dissociation process and the BEP model has failed to predict a good starting point for the TS search. However, in this case, the minimum crossing point of the interaction between the two quadratic surfaces is an acceptable starting point for the TS search.

The CASSCF geometries of the located stationary points and the CASSCF and CCSD(T) relative

energies compare well with recent theoretical results from the literature.[18] The limiting step in the unimolecular decomposition of methyldioxirane is the **1** → **2** ring opening process.

Acknowledgments

Calculations described in this work were performed on an IBM RISC-6000 and a SGI power challenge R10000 at the CID of CSIC and on the IBM SP2 at the CESCA. We thank Prof. Santiago Olivella (Universitat de Barcelona) for his valuable suggestions. The authors also thank Prof. S. D. Peyerimhoff and Dr. M. W. Schmidt for providing a copy of MRD-CI and GAMESS codes, respectively.

References

1. Anglada, J. M.; Besalu, E.; Bofill, J. M.; Crehuet, R. J Comput Chem 1999, 20, 1112–1129.
2. Atkinson, R.; Carter, W. P. L. Chem Rev 1984, 84, 437.
3. Atkinson, R. Atmospher Environ 1990, 24A, 1.
4. Carter, W. P. L. Atmospher Environ 1990, 24A, 481.
5. Atkinson, R.; Aschmann, S. M. Environ Sci Technol 1993, 27, 1357.
6. Horie, O.; Mortgat, G. K. Acc Chem Res 1998, 31, 387.
7. Criegee, R. Angew Chem Int Ed 1975, 14, 745.
8. Herron, J. T.; Huie, E. J Am Chem Soc 1977, 99, 5430.
9. Martinez, R. l.; Herron, J. T. J Phys Chem 1987, 91, 946.
10. Niki, H.; Maker, P. D.; Savage, C. M.; Breitenbach, L. P.; Hurley, M. D. J Phys Chem 1987, 91, 941.
11. Martinez, R. I.; Herron, J. T. J Phys Chem 1988, 92, 4644.
12. Neeb, P.; Horie, O.; Moortgat, G. K. J Phys Chem A 1998, 102, 6778.
13. Karlström, G.; Roos, B. O. Chem Phys Lett 1981, 79, 416.
14. Bach, R. D.; Andrés, J. L.; Owensby, A. L.; Schlegel, H. B.; McDouall, J. J. W. J Am Chem Soc 1992, 114, 7207.
15. Cremer, D.; Gauss, J.; Kraka, E.; Stanton, J. F.; Bertlett, R. J. Chem Phys Lett 1993, 209, 547.
16. Anglada, J. M.; Bofill, J. M.; Olivella; S.; Solé, A. J Am Chem Soc 1996, 118, 4636.
17. Anglada, J. M.; Bofill, J. M.; Olivella, S.; Solé, A. J Phys Chem A 1998, 19, 3398.
18. Cremer, D.; Kraka, E.; Szalay, P. G. Chem Phys Lett 1998, 292, 97.
19. Anglada, J. M.; Crehuet, R.; Bofill, J. M. Chem Eur J 1999, 5, 1809.
20. Roos, B. O. Adv Chem Phys 1987, 69, 399.
21. Anglada, J. M.; Bofill, J. M. Chem Phys Lett 1995, 243, 151.
22. Buenker, R. J.; Peyerimhoff, S. D. Theoret Chim Acta 1975, 39, 217.
23. Buenker, R. J.; Peyenmhoff, S. D.; In: Lowdin, P. O.; Pullman, B., eds. New Horizons of Quantum Chemistry, Vol. 35; Reidel: Dordrecht, 1983; p 183.
24. Buenker, R. J.; Philips, R. A. J Mol Struct Theochem 1985, 123, 291.
25. Curtiss, L. A.; Raghavachari, K.; Trucks, G. W.; Pople, J. A. J Chem Phys 1991, 94, 7221.
26. Hariharan, P. C.; Pople, J. A. Theoret Chim Acta 1973, 28, 213.
27. Cizek, J. Adv Chem Phys 1969, 14, 35.
28. Pople, J. A.; Head-Gordon, M.; Raghavachari, K. J Chem Phys 1987, 87, 5968.
29. Scuseria, G. E.; Schaefer, H. F., III. J Chem Phys 1989, 90, 3700.
30. Krishnan, R.; Binkley, J. S.; Seeger, R.; Pople, J. A. J Chem Phys 1980, 72, 650.
31. Frisch, M. J.; Pople, J. A.; Binkley, J. S. J Chem Phys 1984, 80, 3265.
32. Schmidt, M. W.; Baldrige, K. K.; Boatz, J. A.; Jensen, J. H.; Koseki, S.; Gordon, M. S.; Nguyen, K. A.; Windus, T. L.; Elbert, S. T. QCPE Bull 1990, 10, 52.
33. Frisch, M. J.; Trucks, G. W.; Schlegel, H. B.; Gill, P. M. W.; Johnson, B. G.; Robb, M. A.; Cheeseman, J. R.; Keith, T.; Petersson, G. A.; Montgomery, J. A.; Raghavachari, K.; Al-Laham, M. A.; Zakrzewski, V. G.; Ortiz, J. V.; Foresman, J. B.; Cioslowski, J.; Stefanov, B. B.; Nanayakkara, A.; Challacombe, M.; Peng, C. Y.; Ayala, P. Y.; Chen, W.; Wong, M. W.; Andres, J. L.; Replogle, E. S.; Gomperts, R.; Martin, R. L.; Fox, D. J.; Binkley, J. S.; Defrees, D. J.; Baker, J.; Stewart, J. P.; Head-Gordon, M.; Gonzalez, C.; Pople, J. A. GAUSSIAN, Gaussian, Inc.: Pittsburgh, PA, 1995.
34. Cimiraglia, R.; Ha, T.-K.; Meyer, R.; Günthard, H. H. Chem Phys 1982, 66, 209.
35. Cantos, M.; Merchan, M.; Tomás-Vert, G.; Roos, B. O. Chem Phys Lett 1994, 229, 181.
36. Hammond, G. S. J Am Chem Soc 1955, 77, 334.